# A scanning tunneling microscope for surface science studies

by J. E. Demuth R. J. Hamers R. M. Tromp M. E. Welland

A new design is described for a scanning tunneling microscope intended for surface science studies. The performance of the microscope is evaluated from tunneling images obtained of the Si(111) 7 × 7 surface. Periodic structures, point defects, and grain boundary structures are observed with atomic-scale resolution and are discussed. Illustrations of various types of image processing and data display are presented.

# Introduction

The ability to use electron tunneling between a sample and probe tip in vacuum to obtain information about surfaces heralds a new era in surface science. As demonstrated by Binnig, Rohrer, and co-workers, this method—scanning tunneling microscopy or spectroscopy—has already provided unprecedented insight into numerous surface problems [1-4]. Using a scanning tunneling microscope (STM) one can obtain images of the surface that depend on both structural and electronic features of the surface atoms. The remarkable ability to achieve atomic resolution with this method contrasts strongly with conventional surface science probes which provide a macroscopic average of the

\*\*Copyright 1986 by International Business Machines Corporation. Copying in printed form for private use is permitted without payment of royalty provided that (1) each reproduction is done without alteration and (2) the *Journal* reference and IBM copyright notice are included on the first page. The title and abstract, but no other portions, of this paper may be copied or distributed royalty free without further permission by computer-based and other information-service systems. Permission to *republish* any other portion of this paper must be obtained from the Editor.

microscopic properties one hopes to investigate. The use of the structural and electronic information contained in such tunneling measurements ultimately rests upon understanding numerous details of the tip, the surface, and the tunneling process itself [5–8]. In principle, scanning tunneling studies of well-defined, characterized surfaces—surfaces presumably understood from the last 15 years of modern surface science studies—may provide such information. With this in mind, our efforts are directed towards incorporating an STM into a surface spectroscopy chamber so as to perform both micro- and macroscopic measurements on the same samples.

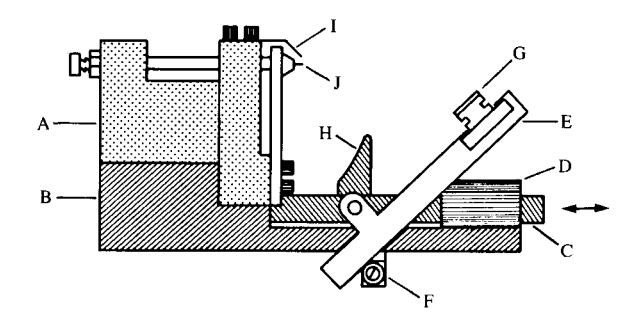
The incorporation of an STM into a conventional surface spectroscopy system so as to permit the routine, flexible operation of each method involves numerous trade-offs. Here we describe a microscope whose features, we believe, make it attractive for a wide range of *in situ* surface studies including other surface spectroscopy techniques. Atomic-scale STM images of the Si(111)  $7 \times 7$  surface have been obtained and are presented to evaluate the microscope's performance. Several interesting features of the surface structure and probe tip are also discussed.

# **Description of the microscope**

The STM we have developed represents a hybrid between the original Binnig et al. [1-4] microscope and the "squeezetunneling" microscope developed by Hansma and coworkers [9]. In the latter, considerable mechanical stability is achieved by having the sample in intimate contact with the probe tip assembly. However, the squeeze-tunneling approach places severe restrictions on the sample

configuration and sample processing needed for UHV surface studies, thereby making it difficult to use directly for surface science studies. Our design accepts conventional surface science samples and allows contact between the sample and the probe tip scanning assembly. We also achieve coarse motion of the sample for transferring and processing in vacuum, as well as fine motion to achieve tunneling, via one simple mechanical assembly. Our design, like that of Pethica and co-workers [10], thereby eliminates the need for a piezoelectric walker or "louse."

A schematic of the microscope is shown in Figure 1. Three orthogonal piezoelectric drives (Vernitron PZT-5A) for scanning the sample are mounted on a two-piece macor support (A) which is attached to a stainless steel base plate (B). On the microscope base plate is a movable carriage consisting of a pair of rods (C) and a stop (H). The carriage is free to move on two sets of ball bushings (D); one pair of ball bushings is mounted within the base plate and is not shown. A horizontal motion of this movable carriage or track is accomplished through a lead screw (not shown) which is coupled to a rotary feedthrough and actuated from outside the chamber. The arms (E) are mounted on pins secured to each of the advance rods (C) and are free to pivot about the pin. When the carriage is moved to the right sufficiently, the arms are forced to pivot by a catch (F) mounted on the base plate. The arms (E) are also springloaded to the movable track so as to maintain a force, thereby pushing the arms counterclockwise into the stop (H). In this way the sample (G) mounted in the arms can be pivoted, upon retraction, well away from the scanning assembly. Such large sample pivoting can allow one to use this microscope as a "flip-manipulator" to observe or process the sample well away from the scanning assembly. When the sample is brought close to the scanning assembly, the stop (H) prevents any further pivoting of the sample, and contact is eventually established between the "foot" (I) and the sample (G). The probe tip is mounted in a miniature collet (J) approximately 0.1 to 0.02 mm behind the foot. The small, light probe tip assembly we use is intended to reduce the inertia as well as increase the resonance frequency of the scanning assembly. Continuing the approach forward, the foot now causes the sample arm to pivot about the foot, thereby demagnifying the carriage motion. The foot-to-probe tip separation of ~0.5 mm and sample-to-pivot distance of 38 mm give a translational reduction of  $\sim$ 70 to 1. This, together with the fine pitch of the lead screw (~1.5 threads/ mm), provides ~250 Å of motion per degree rotation of the lead screw. The spring loading of the sample onto the foot also provides intimate contact with the piezoelectric scanner assembly. Such direct contact between the foot and sample is the main disadvantage of this design and may introduce sample damage and possible contamination. However, this contact area is extremely small and presumably offers reduced sensitivity to vibrations and greater flexibility to



### Figure

Schematic diagram of the scanning tunneling microscope to which this paper pertains: (A) macor block onto which x, y, z piezoelectric scanners are mounted, (B) microscope base plate, (C) carriage rods, (D) ball bushing assembly, (E) connecting arms to sample, (F) catch, (G) sample and sample holder, (H) stop, (I) foot, and (J) probe tip mounted in collet on the x-y piezoelectric drives.

utilize an STM with other techniques, or even, for example, at low temperatures.

The microscope is oriented vertically atop six 4-mm-thick stainless steel plates separated by viton spacers [11] which rest on a platform suspended from a 22.3-cm o.d. flange. (This suspended mounting was intended originally to allow spring mounting of the microscope which was later abandoned in favor of the stacked plates.) Actuation of the carriage motion via the lead screw is performed by a rotary-motion feedthrough mounted to this flange. All electrical connections are made from this flange. The test chamber consists of an ~40-cm-long 15.3-cm o.d. tube mounted vertically to a 220 l/s ion pump. Both are mounted to an airbearing table so as to provide vibrational decoupling from the floor. The entire system is located on the third floor of a steel frame building in an ordinary laboratory.

The feedback control electronics used to control the z piezoelectric motion and maintain a constant tunneling current are functionally identical to those of Binnig et al. [1]. All the piezoelectric drives are controlled using Kepco BOP-1000 programmable power supplies. Two of these supplies, which control the x, y piezoelectric elements, are driven by an IBM PC-XT which is also used for data acquisition. We find that the feedback control response is sufficient that we can mechanically approach the sample to the probe tip to initially establish the tunneling condition without having an accidental contact. During tunneling we can also mechanically adjust the probe-to-sample distance so as to achieve zero voltage on the z piezoelectric drive without causing a collision between the sample and the tip. Such contact or collisions will blunt the probe tip and damage the surface over exceedingly large areas relative to the atomic dimensions one hopes to probe.

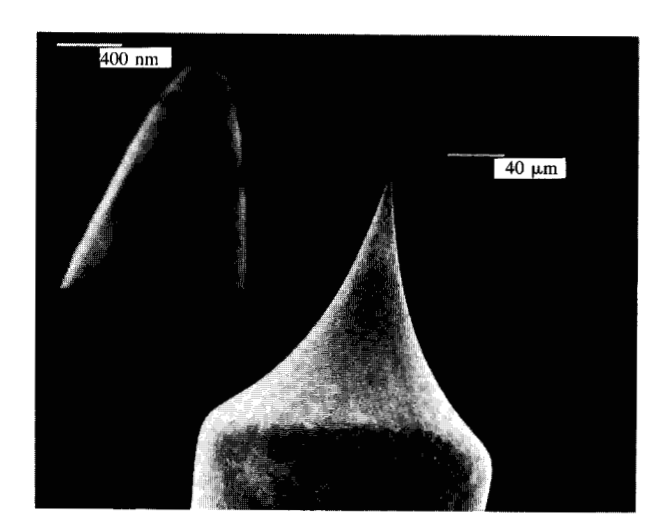
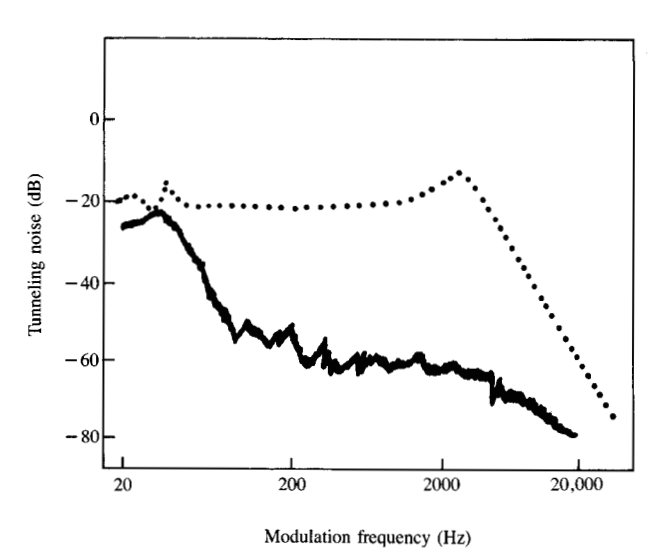


Figure 2

SEM photographs of electrochemically etched tungsten probe tip.



# Figure 3

Spectral analysis of tunneling current noise obtained from an epitaxial Au film. The tunneling current is 2 nA with a 0.3-V bias. The dotted line shows the tunneling noise arising from a 40-meV (p-p) modulation of the bias voltage.

# Sample and tip preparation

We use an electrochemically polished 0.75-mm-diameter drawn tungsten wire for the probe tip, which is manually inserted into the collet attached to the piezoelectric drives. A dc etching in 2M NaOH solution at a bias of 7 V produces very uniform whisker-free tips having a radius of curvature of 1–0.1  $\mu$ m. SEM photographs of a typical etched probe tip

are shown in Figure 2. The insert shows the initial profile of the tip used for the measurements of the Si(111)  $7 \times 7$  surface we discuss later. UHV tip processing utilized in these measurements consists of running  $\frac{1}{2}-1$   $\mu$ A between tip and sample with the sample biased negatively by 50 to 250 V (depending on the radius of the tip). In later studies we have found that this processing is unnecessary and in many cases even detrimental.

The sample we primarily discuss here consists of a 5-mm  $\times$  12-mm section of Si(111) wafer (n-type 0.1–0.2  $\Omega$ -cm) which is secured to the sample holder at two ends and resistively heated. One advantage of our microscope's sample-holding assembly is its all-metal construction, which allows more rapid conduction of heat from the sample and thermal equilibration after processing. Sample cleaning is performed in several stages of annealing designed to degas the sample and sample holder. Final sample cleaning is carried out by rapidly heating the Si wafer momentarily to 1100°C to "flash off" the passivating/protecting oxide layer. The ambient background pressure during this processing remains in the low to mid-10<sup>-8</sup> Pa range while system base pressures are typically in the low 10<sup>-9</sup> Pa range. Such a sample-cleaning procedure has been shown to be highly reproducible with LEED, Auger, and MEIS [12] and has also yielded well-resolved surface states in UPS which are believed to be characteristic of good  $7 \times 7$  surfaces [13]. The present chamber contains no other ways to characterize the sample.

# Microscope performance and illustrative results

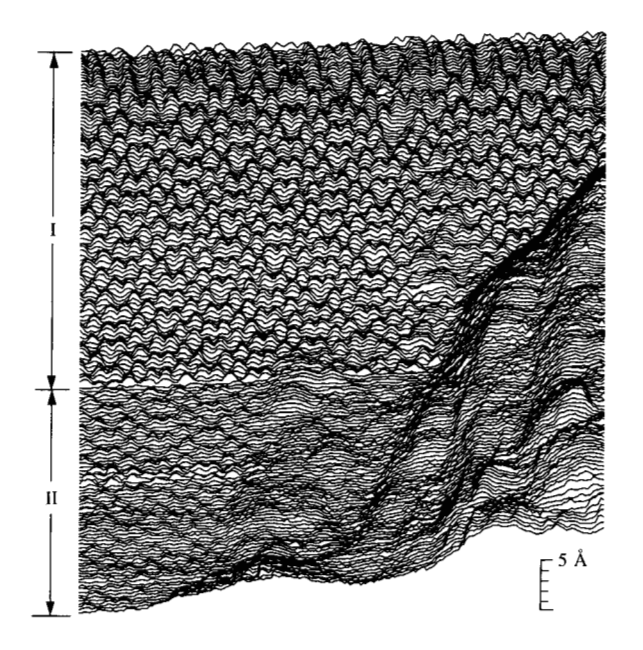
Numerous tests have been performed to understand the performance and limitations of this design. One important consideration for scanning is the mechanical resonances of the piezoelectric drive system, which can introduce extra noise or cause tip-surface contact to occur when scanning rapidly. This is particularly true of the z piezoelectric drive when rapid contour or topology changes occur on the surface. As a simple test for resonances associated with the z piezoelectric drive motion, we have performed a spectral analysis of the tunneling current while modulating the tunneling bias voltage. In Figure 3 we show the noise spectrum during tunneling (solid line) relative to that produced by modulating the bias voltage (dotted line) at the same frequency as the spectral analysis (i.e., an external output for the spectrum analyzer frequency is used to drive the bias voltage). Mechanical resonances as well as instabilities in the loop controller are expected to produce peaks and structure in the noise spectrum. Some weak resonances are seen near 20 and 40 Hz (possibly associated with the wires on the drives) and a major resonance at about 3 kHz. The marked attenuation above about 4 kHz seen in Figure 3 occurs from the roll-off of the head amplifier in these studies. The main resonance for the piezoelectric scanner assembly is found by directly modulating the x and

y drives while tunneling. This occurs at 7 kHz, with weaker resonances at 2 and 3.3 kHz. We attribute these relatively high resonance frequencies to the sturdy macor mounting assembly we have used and our rigid mounting of the drives to it. The breadth of the 3-kHz resonance we find in Figure 3 can be attributed to the heavy (0.5-mm-diameter) gold wire connected to the probe tip, which acts to dampen the vibrations of the scanner assembly.

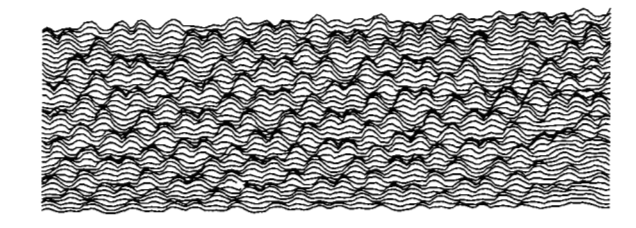
A better test of the microscope's performance is the overall noise level and topological detail we can achieve on a well-defined surface. In Figure 4 we show a 250-  $\times$  250-Å set of line scans of a portion of a Si(111)  $7 \times 7$  surface. A data point is taken every 1.25 Å along a scan row and successive rows are offset by 1.25 Å. Here a 2-V positive bias is applied to the sample and the tunnel current set to 1 nA. The scan shows an inclined nonperiodic region in the lower right-hand corner and two regions of 7 × 7 structures labeled as I and II. The top two thirds of scan region I shows the largest corrugations, while the lower third shows smaller corrugations and more noise. The differences between regions I and II arise from a small change in the structure of the tip during scanning. The fact that we see a small (~4 Å) lateral shift in the registry of the  $7 \times 7$  structure between regions I and II, as well as a small (0.5-Å) decrease in the tipto-sample distance, suggests atomic-scale rearrangement of the tip. For example, a cluster of tungsten (or silicon) atoms at the apex of the probe tip may have been atomically rearranged by a very slight contact to the surface or by the transfer [14] of a chemically active atom which reacts to change the tip configuration. The reduced corrugation also suggests a "blunter" tip, where tunneling may occur from a cluster of atoms instead of just one. We have also observed an image characteristic of tunneling from two points on the tip which produces a streaked doublet of structures for every feature of the  $7 \times 7$  surface. Fortunately, this tip condition appears to occur seldom (for <2% of the tips used to date).

The noise we find in our data is very low and consists mostly of noise spikes. In region I they have amplitudes of  $\sim 0.15$  Å and are consistent with the present electrical noise in our data acquisition system. More "noise" appears to be present in the amorphous region. The quality of our tunneling topograph is seen better in Figure 5, which shows a  $190-\times65$ -Å section of the  $7\times7$  surface.

An important aspect of tunneling microscopy is displaying the data in a form that allows detailed visual inspection and timely analysis of the data. In Figure 6(a) we show a gray-scale image of some of the data. Here the lighter intensity corresponds to atoms or wavefunctions sticking out of the surface. In Figure 6(b) we show the same data in a map-maker's color scale. The use of color allows one to readily distinguish small topological features such as the small depressions between the high spots. In order to eliminate the small angular misorientations of the scanning piezoelectric elements relative to the plane of the surface (e.g., visible in

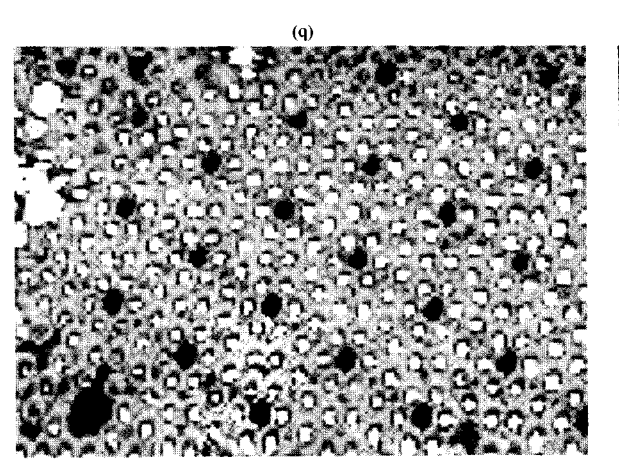


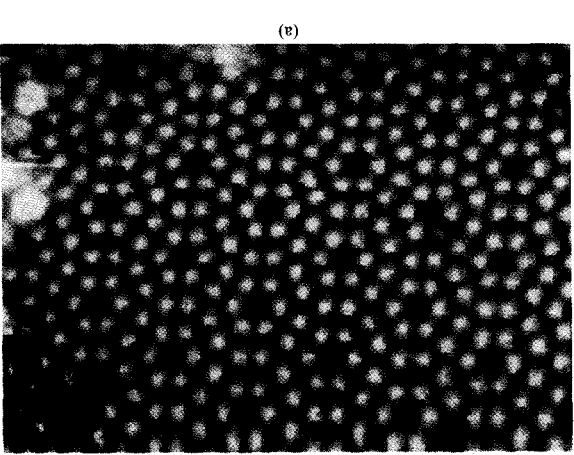
Topographical scan of a 250  $\times$  250-Å region of a Si(111) 7  $\times$  7 surface. The scale corresponds to the vertical displacement of the z piezoelectric drive required to maintain a constant tunneling current.



Topographical scan of a 190  $\times$  65-Å region of Si(111) 7  $\times$  7 surface. The data points here were taken at 1.25-Å intervals in this line scan and are linearly connected (not curve fit).

Figures 4 and 5 as a slight inclination of the line scans), we have fitted parts of the image to an average plane which is then subtracted off. The skewing of the  $7 \times 7$  unit cell in Figure 6 arises from piezoelectric "creep" and possible thermal drift which occurs during the scan. This amounts to typically  $\sim 0.6$  Å per minute and is accounted for by shifting the rows to produce the expected symmetry of the  $7 \times 7$  unit cell. Such an "adjusted" image of a portion of region I of Figure 4 is shown in Figure 7(a). Here no averaging or noise





(a) Gray-scale and (b) color-scale image of a 175 × 115-Å region of Si(111) 7 × 7 surface after a uniform background correction.

shown a depletion of carriers (and electrically active dopants) at the surface of n-type, As-doped Si [17]. The detailed nature and origin of these missing adatoms are thereby still unclear. They may be native defects or may be associated with some subsurface contaminant such as carbon or

surface. they seldom occur and cover only a minute fraction of the sample cleanliness during processing: On our best samples amorphous regions correlates well to the vacuum and grain boundary. We note that the occurrence of these structures where the inclined amorphous region "pins" the arises from the nucleation and growth of two separate  $7 \times 7$ dislocation tilted out of the surface. Such a misht likely defect is a surface misht dislocation rather than a bulk differences across this line defect, which indicates that this Surprisingly, we see no evidence for topographical height along this grain boundary and appears to decorate it. amorphous region also seems to be preferentially located this area reveals a surface grain boundary. Part of the alignment of the deep minima of the  $7 \times 7$  structure near region in the lower right-hand corner. A comparison of the 7 is an extended defect arising to the left of the inclined The second interesting imperfection in the image in Figure

In summary, we have described a new type of scanning tunneling microscope which combines a piezoelectric scanner as utilized by Binnig et al. [1] with a rugged, totally mechanical sample approach assembly that establishes intimate contact between the sample and scanner assembly. The stability, noise, and overall performance of this

Summary

reduction has yet been made. Figure 7(b) has been Fourier-filtered to remove spurious "high-frequency" noise. Further display of the tunneling image after interpolating between data points and using false color produces even greater and 7(a-c) allows one to compare directly the various ways of processing and presenting the data.

The images of the Si(111) 7 × 7 surface shown in Figures.

do not arise from boron or bulk doping. In fact, recent EELS However, our results on n-type Si indicate that these features and corresponds well to that found previously [15]. spacing we find between these three defects is  $\sim 5$  unit cells that expected on the basis of the bulk doping [15]. The at the surface enhanced by four orders of magnitude over [15]. The number of these suggested a boron concentration and were associated with boron dopant atoms on the surface Similar missing adatoms were observed in previous studies region of the  $7 \times 7$  unit cell, well away from the deep hole. adatoms are similar in that they are located in the central have been associated with adatoms [2, 14]. All missing corners, we observe missing protrusions. These protrusions Figure 7 as well as in the upper left and extreme right-hand information. First, in the lower right corner of the image in images also show several imperfections which convey new to be a result of the differences in bias voltages used. Our of the unit cell than that seen previously [2], which we find smaller difference in height between the right and left sides similar to those found earlier [2, 15]. We find a much maximum corrugation amplitudes we observe are also Binnig et al. [2] as well as more recent results [15, 16]. The o and 7 are in general agreement with the original results of The images of the  $Si(111) 7 \times 7$  surface shown in Figures

studies on thermally annealed  $Si(111) \times 7$  surfaces have

microscope have been evaluated using topographic scans of the Si(111)  $7 \times 7$  surface. These images are found to be comparable to all previous results on the Si(111)  $7 \times 7$  surface and demonstrate a lateral resolution of 5 Å and vertical resolution of  $\sim 0.1$  Å. We also present various ways of processing and presenting the STM data to readily examine atomic-scale features. In particular, we observe point defects in the Si(111)  $7 \times 7$  surfaces as well as a surface misfit boundary between two  $7 \times 7$  structures. The ability to study such nonperiodic structures and imperfections represents another of the many novel capabilities of scanning tunneling microscopy.

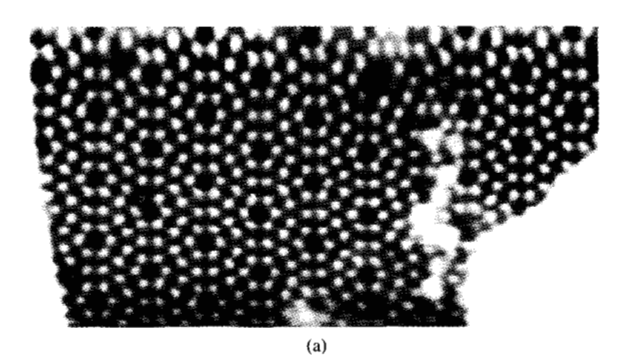
# **Acknowledgments**

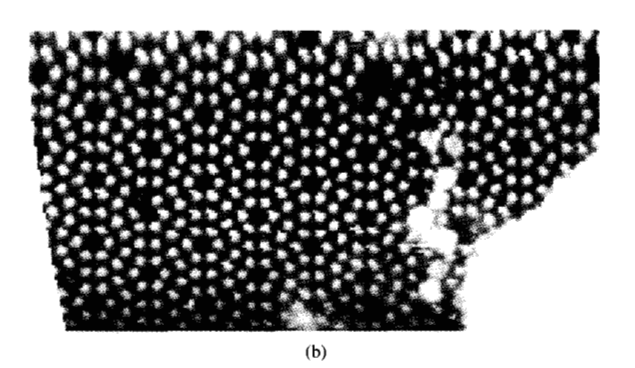
The authors would like to acknowledge P. Schroer for technical assistance in the design and construction of the control electronics, computer interface, and software systems; W. Kahn, A. Moldovan, F. Babbage, and H. Gertling for machining many of the parts; C. Aliotta for the SEM work; and E. J. Farrell and W. Krakow for assistance in image processing. Useful discussions with R. Feenstra and J. Golovchenko are gratefully acknowledged.

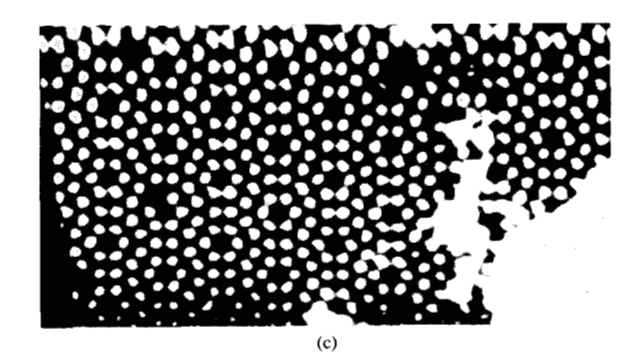
### References and note

- 1. G. Binnig and H. Rohrer, Helv. Phys. Acta 55, 726 (1982).
- G. Binnig, H. Rohrer, Ch. Gerber, and E. Weibel, Phys. Rev. Lett. 50, 120 (1983).
- G. Binnig, H. Rohrer, Ch. Gerber, and E. Weibel, *Phys. Rev. Lett.* 49, 57 (1982).
- G. Binnig, H. Rohrer, Ch. Gerber, and E. Weibel, Surf. Sci. 131, 37a (1983); 144, 321 (1984).
- 5. J. Tersoff and D. R. Hamann, Phys. Rev. Lett. 50, 1998 (1983).
- N. Garcia, C. Ocal, and F. Flores, Phys. Rev. Lett. 50, 2002 (1983).
- 7. A. Baratoff, Physica 127B, 137 (1984).
- A. Selloni, P. Carnevali, E. Tosatti, and C. D. Chen, *Phys. Rev.* B 31, 2602 (1985).
- J. Moreland, S. Alexander, M. Cox, R. Sonnenfeld, and P. K. Hansma, Appl. Phys. Lett. 43, 387 (1983); J. Moreland and P. K. Hansma, Rev. Sci. Instrum. 55, 399 (1984).
- M. D. Pashley, J. B. Pethica, and J. Coombs, Surf. Sci. 152, 27 (1985).
- This vibration isolation system is further described by G. Binnig and H. Rohrer, IBM J. Res. Develop. 30, pp. 355-369 (1986, this issue).
- 12. R. M. Tromp and E. J. Van Loenen, Surf. Sci. 156, 441 (1985).
- F. J. Himpsel, *Physica* 117B and 118B, 767-770 (1983) and references therein.
- For example, see Robert Gomer, IBM J. Res. Develop. 30, pp. 428-430 (1986, this issue).
- G. Binnig, H. Rohrer, F. Salvan, Ch. Gerber, and A. Baró, Surf. Sci. 152, 17 (1985).
- R. S. Becker, J. Golovchenko, and B. S. Swartzentruber, *Phys. Rev. Lett.* 54, 2678 (1985).
- 17. Joseph A. Stroscio and W. Ho, Phys. Rev. Lett. 54, 1573 (1985).

Received July 1, 1985; accepted for publication October 24, 1985







Processed tunneling images of a 210  $\times$  115-Å portion of the region of Si(111) 7 x 7 surface shown in Figure 4: (a) adjusted gray-scale image, (b) Fourier-filtered gray-scale image, and (c) false-color image. The full range of the gray-scale images corresponds to a vertical change in distance of 2.0 Å.

Joseph E. Demuth IBM Research Division, P.O. Box 218, Yorktown Heights, New York 10598. Dr. Demuth is manager of the interface physics group at the Thomas J. Watson Research Center. He received a B.S. degree in physics from Rensselaer Polytechnic Institute in 1968 and a Ph.D. degree in applied physics from Cornell University in 1973. His research activities have focused on the use and development of surface-sensitive techniques for surface science studies including LEED, UV photoemission, surface-enhanced Raman, and high-resolution electron energy loss spectroscopy. He has over 100 publications concerning bonding, geometric and electronic structure, and chemical reactions on both metal and semiconductor surfaces. His current interests involve the use of

scanning tunneling microscopy to understand the local chemical and physical properties of semiconductor surfaces and interfaces. He is a member of the American Physical Society and Sigma Xi, and is currently chairman of the Surface Science Division of the American Vacuum Society.

Robert J. Hamers IBM Research Division, P.O. Box 218, Yorktown Heights, New York 10598. Dr. Hamers is a visiting scientist at the Thomas J. Watson Research Center, where he has worked since February 1985. At IBM, he has been engaged mainly with the actual STM operation and with improving its stability and noise characteristics. Dr. Hamers received a B.S. in 1980 from the University of Wisconsin. He received an M.S. in 1982 and a Ph.D. in 1985, both in chemistry, from Cornell University, where he applied laser techniques to study energy transfer in molecule-surface collisions.

Rudolf M. Tromp IBM Research Division, P.O. Box 218, Yorktown Heights, New York 10598. Dr. Tromp received his Ph.D. (cum laude) in physics from the University of Utrecht in 1982. His thesis work, performed at the FOM Institute for Atomic and Molecular Physics (Amsterdam, The Netherlands) was concerned with the structure of silicon surfaces. For these studies he received the 1981 Wayne B. Nottingham Award at the 41st Annual Conference on Physical Electronics in Montana. In 1983 he joined the IBM Thomas J. Watson Research Center to perform studies on the structure of surfaces and interfaces. He is presently working on scanning tunneling microscopy and medium-energy ion scattering.

Mark E. Welland Electrical Engineering Department, Cambridge University, Trumpington Street, Cambridge, England CB2 1PZ. Dr. Welland is a University Lecturer in electrical engineering at Cambridge University, and a Fellow of St. John's College, Cambridge. He received a B.Sc. in physics from Leeds University in 1978 and an M.Sc. and a Ph.D. in physics from Bristol University in 1979 and 1982, respectively. His Ph.D. thesis was an electron microscopy study of fracture mechanisms in copper and copper-bismuth. He held a postdoctoral position at Bristol University and at the Max-Planck Institute, Munich, Federal Republic of Germany, from October 1982 to May 1984. From that time until September 1985, he participated in the study described in this paper and related investigations as a Visiting Scientist at the IBM Thomas J. Watson Research Center. Dr. Welland's current research efforts are in scanning tunneling microscopy.